Journal of Experimental Botany, Vol. 59, No. 6, pp. 1201–1213, 2008
doi:10.1093/jxb/ern027 Advance Access publication 20 March, 2008
This paper is available online free of all access charges (see http://jxb.oxfordjournals.org/open_access.html for further details)

Journal of Experimental Botany
www.jxb.oxfordjournals.org

RESEARCH PAPER

The *AtMYB11* gene from *Arabidopsis* is expressed in meristematic cells and modulates growth *in planta* and organogenesis *in vitro*

Katia Petroni[1], Giuseppina Falasca[2], Valentina Calvenzani[1], Domenico Allegra[1], Carmine Stolfi[2], Luana Fabrizi[2], Maria Maddalena Altamura[2] and Chiara Tonelli[1,*]

[1] *Dipartimento di Scienze Biomolecolari e Biotecnologie, Università degli Studi di Milano, Via Celoria 26, I-20133 Milano, Italy*

[2] *Dipartimento di Biologia Vegetale, Università La Sapienza, Piazzale Aldo Moro 5, I-00185 Roma, Italy*

Received 8 August 2007; Revised 18 January 2008; Accepted 21 January 2008

Abstract

In plants, MYB transcription factors play important roles in many developmental processes including cell cycle progression, cell differentiation, and lateral organ polarity. It is shown here that the *R2R3-MYB AtMYB11* gene is expressed in root and shoot meristems and also in young still meristematic leaf and flower primordia of *Arabidopsis*. Knock-out *atmyb11-I* mutants and RNAi plants germinate faster, show a faster hypocotyl and primary root elongation, develop more lateral and adventitious roots, show faster development of the inflorescence, and initiate more lateral inflorescences and fruits than wild-type plants. The opposite phenotype was displayed by plants overexpressing *AtMYB11*. *De novo* formation of root meristemoids and, consequently, macroscopic roots, from thin cell layers cultured *in vitro* was enhanced in explants from *atmyb11-I* and reduced in those from lines overexpressing *AtMYB11*. These findings indicate that *AtMYB11* modulates overall growth in plants by reducing the proliferation activity of meristematic cells and delaying plant development.

Key words: Arabidopsis, *AtMYB11*, growth rate, meristems, thin cell layers.

Introduction

MYB proteins are transcription factors with a specific DNA-binding domain comprising up to three imperfect tandem repeats (R1, R2, R3), each of about 52 residues, that fold into a helix-turn-helix motif. In vertebrates, the *MYB* gene family is small and includes *c-MYB*, *A-MYB*, and *B-MYB*; the products of these genes are involved in the control of cell proliferation, differentiation, and apoptosis (Weston, 1998). In plants, the *MYB* family is much more extensive: at least 198 *MYB* genes have been identified in Arabidopsis (Yanhui *et al*., 2006). Plant MYB proteins are classified according to the number of MYB repeats. Those with R1R2R3 are the most similar to their vertebrate counterparts; those with R2R3 constitute the largest group and are plant-specific; those with a single MYB domain, or variants of it, are known as MYB-related proteins (Stracke *et al*., 2001; Petroni *et al*., 2002; Yanhui *et al*., 2006). The plant *MYB* genes characterized so far are involved in a wide range of processes including cell cycle progression, cell differentiation, lateral organ polarity, flower and seed development, and secondary metabolism; as well as defence and stress responses, light and hormone signal transduction, and the circadian clock (Petroni *et al*., 2002; Yanhui *et al*., 2006).

Various R1R2R3-MYB transcription factors have been shown to control cell proliferation in cell cultures. The MYB-related *AtCDC5* gene of *Arabidopsis* is able to complement the growth-defective phenotype of a *cdc5* temperature-sensitive *Saccharomyces pombe* mutant, restoring the G_2/M transition (Hirayama and Shinozaki, 1996). The MYB-related *NtMYBA1*, *NtMYBA2*, and *NtMYBB* genes control G_2/M transition in tobacco by modulating the expression of B-type mitotic cyclin genes and other co-expressed genes by binding to an MSA-element, required to G_2/M phase-specific timing of expression (Ito *et al*., 2001). A new MYB-related transcription

* To whom correspondence should be addressed. E-mail: chiara.tonelli@unimi.it

© 2008 The Author(s).
This is an Open Access article distributed under the terms of the Creative Commons Attribution Non-Commercial License (http://creativecommons.org/licenses/by-nc/2.0/uk/) which permits unrestricted non-commercial use, distribution, and reproduction in any medium, provided the original work is properly cited.

factor and a Myc-type protein have been identified as possible regulators of cyclin *AtCYCB1;1* in *Arabidopsis* (Planchais *et al*., 2002). However, the role of these genes in plant development remains poorly understood.

Local control of cell proliferation has been attributed to *R2R3-MYB* orthologous genes which control lateral organ polarity, including *RS2* from maize, *AS1* from *Arabidopsis*, and *PHAN* from *Antirrhinum majus* (Waites *et al*., 1998; Timmermans *et al*., 1999; Byrne *et al*., 2000). PHAN seems to control organ growth by modulating the expression of *CycD3a* cyclin in leaf and flower primordia (Towers *et al*., 2003). In addition, some *R2R3-MYB* genes are involved in the formation of lateral meristems, including the tomato *BLIND* gene and its *Arabidopsis* orthologues *RAX1-3* (Schmitz *et al*., 2002; Keller *et al*., 2006; Muller *et al*., 2006).

It is shown here that *AtMYB11* is expressed in *Arabidopsis* apical, lateral, and adventitious meristems and in young still meristematic organ primordia. Knock-out *atmyb11-I* plants are similar to wild-type plants, but show accelerated germination and morphogenesis, increased rates of leaf and lateral root initiation, faster development of the inflorescence, and enhanced rooting response in *in vitro* culture. Conversely, plants overexpressing *AtMYB11* have reduced growth compared to wild-type and *atmyb11-I* plants, and showed a reduced rooting response *in vitro*. Our data indicate that *AtMYB11* modulates overall growth in plants by reducing proliferation activity in all types of meristematic cells and delaying plant development.

Materials and methods

Plant material and growth conditions

Arabidopsis ecotypes used were *Columbia* (*Col*) for transgenic plants (*pMYB11::GUS*, *RNAi::MYB11*, and *35S::MYB11*) and *Landsberg erecta* (*Ler*) for *atmyb11-I*. Wild-type segregants of mutants and transgenics were used as controls in all experiments. Seed lots to be compared were harvested the same day from plants grown at the same time in the same environmental conditions and stored at 4 °C in plastic tubes. Germination assays were performed in triplicate using seeds obtained from two independent sowings of the seed sets to be compared. Seeds were sterilized and sown on half-strength MS (Sigma) supplemented with 0.55 mM myo-inositol, 0.3 μM thiamine-HCl, 2% (w/v) glucose, and 0.8% agar (w/v, Sigma), in long day conditions (16/8 h light/dark) at a fluence rate of 80 μE m^{-2} s^{-1} and 22±2 °C. Differences in growth parameters were evaluated as mean size increases (±SE) per 12 h intervals and as mean values and percentages (±SE) d^{-1}, and statistically compared using Student *t* test.

Semi-quantitative RT-PCR analysis

Total RNA was isolated (van Tunen *et al*., 1988) from organs harvested at various stages as previously described (Gusmaroli *et al*., 2001). Approximately 5 μg were reverse-transcribed using RT Superscript II (Invitrogen) and an oligo dT, as previously described (Procissi *et al*., 1997). After first strand cDNA synthesis, samples were diluted 50 times and used as templates for semi-quantitative RT-PCR, with *AtMYB11*-specific primers Z17F2 (5′-GCCAATACCGTCGAGAATGCGCC-3′) and Z17R3 (5′-TCGTC-AATATCCAACGGTTCTCC-3′) and *TSB1*-specific primers TSB1-F1 (5′-CTCATGGCCGCCGGATCTGA-3′) and TSB1-R1 (5′-CT-TGTCTCTCCATATCTTGAGCA-3′) as a control of cDNA concentration (Berlyn *et al*., 1989; Procissi *et al*., 1997). The amplifications were carried out within linear ranges (25 cycles). The PCR products were transferred onto Hybond N^+ nylon membranes (Amersham) and hybridized with gene-specific probes labelled using the DIG-High Prime kit (Roche). Nested PCR re-amplifications were also performed for an additional 35 cycles on specific samples (Fig. 1A, lower panel), using the *AtMYB11*-specific primers Z17F3 (5′-AAGAACCAGCAGATCCGCCATGA-3′) and Z17R4 (5′-TGGAGTCCCTTTGTCTGATCTC-3′).

In situ *hybridization*

Flowers and siliques were collected at various developmental stages from 7-week-old plants grown on soil. Seedlings grown on MS agarose plates supplemented with 1% sucrose were collected at 4 days after germination (DAG). Samples were immediately fixed in freshly prepared 4% (w/v) *p*-formaldehyde in phosphate buffered saline (130 mM NaCl, 7 mM Na_2HPO_4, 3 mM NaH_2PO_4) under vacuum for 3 h. The fixed material was placed in 70% ethanol and stored at 4 °C pending processing. Embedding procedures were performed as previously described (Procissi *et al*., 1997), except that each step was reduced to 1 h. The template for the *in situ* hybridization probe was prepared as described in the Lig'nScribe PCR Promoter Addition Kit (Ambion, USA). A PCR fragment obtained with the primers Z17F2 and Z17R3 (see above) was ligated non-directionally to a T7 promoter adapter as recommended by Ambion. The template for the antisense strand *AtMYB11* probe was generated by PCR using an aliquot of the ligation reaction using Z17F2 and the Ambion PCR primer 1 (5′-GCTT-CCGGCTCGTATGTTGTGTGG-3′). Z17R3 and Ambion PCR primer 1 were used to generate the template for the sense strand *AtMYB11* probe. Sense and antisense DIG-11-UTP labelled RNA probes were synthesized with T7 RNA polymerase using components from Boehringer. Eight μm-thick tissue sections were cut and mounted on poly-L-lysine-coated slides and the *in situ* hybridization carried out as previously described (Coen *et al*., 1990). Immunological detection of the hybridized probe was carried out as described in the Boehringer digoxigenin-nucleic acid detection kit. For visualizing the red hybridization signal, sections were viewed under dark-field conditions using an Axioscope light microscope (Zeiss) and photographed using a Zeiss camera with a Kodak Ektachrome 100 PLUS film. Digital images were acquired with a scanner CanoScan 2700F.

Isolation of atmyb11-I *mutant and Southern analysis*

The *atmyb11-I* mutant allele in the *Ler* ecotype has previously been isolated by PCR screening of the S3 generation of Wageningen *Arabidopsis En-I* lines (Speulman *et al*., 1999), using the *AtMYB11*-specific primer Z17R3 (see above) in combination with primers Itr2 and Itr3, complementary to the 5′ and 3′ terminal inverted repeats, respectively, of the *I* transposon as previousy described (Meissner *et al*., 1999). To generate a stable mutant, the progeny of the positive plant were outcrossed with the wild-type *Ler* ecotype to segregate the *T-En5* transposase source (Meissner *et al*., 1999). F_2 segregants free of *T-En5* transposase were selected using a PCR screen, as previously described by Speulman *et al*. (1999).

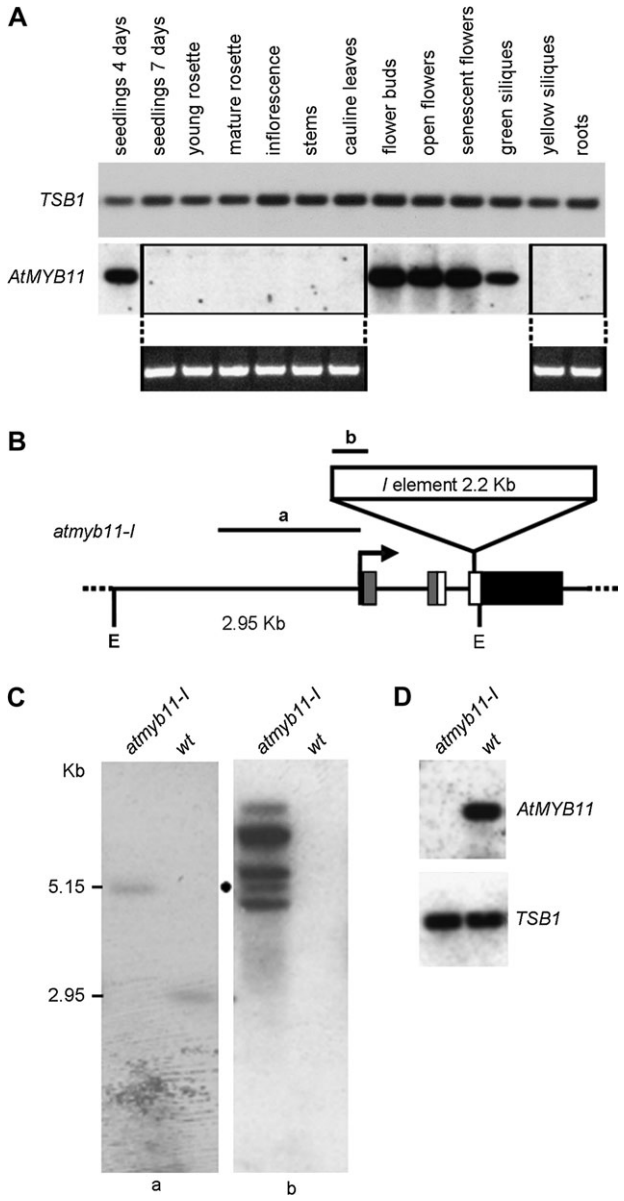

Fig. 1. RT-PCR of *AtMYB11* expression and isolation of *atmyb11-I* knock-out mutant. (A) RT-PCR analysis showing transcript level of *AtMYB11* and the *tryptophan synthase1* β *subunit* (*TSB1*) control gene in indicated organs (25 cycles). PCR products were blotted and hybridized with random primed probes (top and middle panels). PCR products highlighted with open boxes were re-amplified with nested primers (see methods) for 35 additional cycles (lower panel). (B) Structure of *AtMYB11* gene and position of *I* element. The black right-angled arrow indicates the ATG. The positions of DNA-binding R2 and R3 repeats are indicated by grey and open boxes, respectively. The black box indicates the 3′ specific coding region. Black bars indicate a 1179 bp promoter fragment from *AtMYB11* (a) and a 267 bp fragment from the left border of the *I* element (b) used as probes in Southern analysis (C). E indicates *Eco*RI restriction sites. (C) Southern blot analysis of genomic DNA of *Ler* ecotype (wt) and mutant plants (*atmyb11-I*) digested with *Eco*RI and hybridized with a 1179 bp promoter fragment from *AtMYB11* (a) and *I* fragment (b) as probes (see B). In the *atmyb11-I* mutant in (a), a 5.15 kb *Eco*RI fragment derived from the insertion of the *I* transposon in *AtMYB11* (black dot) was observed. Four *Eco*RI fragments in addition to the 5.15 kb *Eco*RI fragment were detected in (b), indicating that there are additional independent *I* insertions. (D) RT-PCR analysis of expression of *AtMYB11* transcripts in *Ler* (wt) and *atmyb11-I* seedlings, indicating the absence of the *AtMYB11* transcript in the *atmyb11-I* mutant. PCR products were blotted and hybridized with random primed probes. The *tryptophan synthase1* β *subunit* (*TSB1*) gene was used as a control.

Genomic DNA was extracted from *Ler* ecotype and *atmyb11-I* mutant plants as previously described (Galbiati *et al*., 2000). DNA was digested with *Eco*RI, separated by agarose gel electrophoresis, blotted and hybridized as previously described (Dellaporta and Moreno, 1994). As probes, the 1179 bp promoter fragment from *AtMYB11* described above and a 267 bp fragment up to a *Sal*I restriction site containing the 5′ end of the *I* element (Aarts *et al*., 1995) were used to detect *I* element insertions.

Constructs and generation of transgenic lines

The *pAtMYB11::GUS* fusion was constructed from a 1179 bp genomic fragment amplified by PCR with a forward primer containing a *Hin*dIII restriction site at the 5′ end (5′-AAGCTTAACCAATCAGGATTAAG-3′) and a reverse primer containing a *Sma*I restriction site at the 3′ end (5′-CCCGGGAAAATCACTCACTTCACT-3′). The PCR fragment was cloned in the pCR4-TOPO (Invitrogen), excised with *Hin*dIII-*Sma*I and subcloned between the *Hin*dIII-*Sma*I sites preceding the *GUS* gene in the binary vector pGPTV-Kan (Becker *et al*., 1992). The construct for *35S::MYB11* lines was obtained as follows: *AtMYB11* cDNA was amplified by PCR (Z17F8 5′-TCGCCGGCCGAGAGAATGGGA-3′ and Z17R15 5′-AATCTTTCAAGACAAAAGCCAAG-3′), cloned in pCRII-TOPO (Invitrogen) and sequenced. A *Bam*HI-*Xba*I fragment containing full-length *AtMYB11* cDNA was excised and subcloned in pRTΩ/Not/Asc (Uberlacker and Werr, 1996). The overexpression cassette was then excised with *Asc*I and subcloned in the pGPTV-Kan-Asc vector. The construct for *RNAi::MYB11* lines was obtained as follows: an *AtMYB11*-specific PCR fragment was amplified with primers Z17F2 and Z17R3 modified with *att*B sequences at the ends to create an entry vector in pDONR™207 (Invitrogen) and then recombined into pFGC5941 (www.ChromDB.org).

Constructs were introduced into *A. tumefaciens* GV3101 (Labereke *et al*., 1974) and transferred to *Col* by the floral dip method (Clough and Bent, 1988). Homozygous T_3-independent lines with a single T-DNA insertion were selected by segregation analysis on MS agar plates supplemented with 1% (w/v) sucrose containing 50 μg ml^{-1} kanamycin (*pAtMYB11::GUS* and *35S::MYB11*) or 50 mM BASTA® AgrEvo (*RNAi::MYB11*).

GUS staining and histology

The *pAtMYB11::GUS* transgenic plants were harvested daily from sowing up to the mature silique stage, exposed to the GUS staining procedure for 16 h, cleared and examined as previously described by Cominelli *et al*. (2005) or cleared as described by Malamy and Benfey (1997), observed using Nomarski optics on a Zeiss Axio Imager.D1 microscope with a video camera Axiocam MRc5. Alternatively, GUS-stained material was fixed in 70% (v/v) ethanol, embedded, and sectioned as described for the *in situ* analysis. For the other histological analyses, seedlings and thin cell layers (TCLs) were fixed in 70% (v/v) ethanol, embedded in Technovit 7100 (Heraeus Kulzer), sectioned at 4 μm intervals and stained with 0.05% (w/v) toluidine blue. Histological sections were examined under a DAS Leica DMRB microscope with a DC500 video camera. Measures were carried out with a personal computer (Optiplex GX 240MT) using the Leica IM1000 IMAGE ANALYSIS software and the means (±SE) compared using the Student *t* test.

In vitro *culture of thin cell layers*

Superficial thin cell layers (TCLs, 5×3 mm, six cell layers including the epidermis) were excised from the inflorescence stem internodes of 35-d-old plants of *atmyb11-1*, *35S::MYB11*, and the corresponding wild-type ecotype (*Ler* for *atmyb11-I* and *Col* for *35S::MYB11*). One hundred TCLs per genotype were cultured for 30 d on medium consisting of Murashige and Skoog (1962) salts supplemented with 0.55 mM myo-inositol, 0.1 μM thiamine-HCl, 1% (w/v) sucrose, 0.8% agar (w/v, Sigma) (pH 5.8), and with 10 μM indole-3-butyric acid (IBA) and 0.1 μM kinetin (kin), under continuous darkness, at 24±2 °C, according to Falasca *et al.* (2004). The analysis of the rooting response was conducted under a dissecting microscope (MZ8 LEICA stereomicroscope) at the end of the culture period. The experiments were repeated three times (100 explants per replicate) without significant differences in the percentage of rooting explants (χ^2 test). The response was quantified as the mean percentage (±SE) of TCLs that had rooted in the three replicates. The differences between the means were evaluated using Student *t* test. The images of TCLs were acquired in digital form with a colour video camera (LEICA DC500) applied to the stereomicroscope. The experiments were repeated three times with similar results.

Results

AtMYB11 *is expressed in meristematic cells*

In order to determine the function of *AtMYB11* in *Arabidopsis*, its expression pattern was first analysed in different organs and developmental stages. RT-PCR showed that *AtMYB11* is mainly expressed in 4-d-old seedlings and throughout flower development, but increasing the number of cycles the *AtMYB11* transcript was detected at very low levels in all vegetative organs (Fig. 1A).

The cellular and tissue distribution of *AtMYB11* was further investigated by *in situ* hybridization experiments on seedlings, flowers, and seeds (Fig. 2). In 4-d-old seedlings, the *AtMYB11* transcript was mainly present in shoot apical meristem (SAM) and meristematic leaf primordia (Fig. 2E and inset). During flower development, *AtMYB11* was expressed in inflorescence meristem and in the still meristematic floral organ primordia (Fig. 2A, bud at stage 6 according to Smyth *et al*., 1990), but as the latter developed into complete flowers, the transcript became essentially confined to ovule primordia (Fig. 2B). After anthesis, *AtMYB11* was found in fertilized ovules developing into seeds and in the ovary wall developing into silique wall (Fig. 2C). In the mature embryo, the transcript was mainly located close to the protoderm and the root pole (Fig. 2D). Similar hybridization experiments performed with the sense probe gave no signal (not shown).

Additional information was obtained from transgenic plants carrying a 1179 bp promoter fragment of *AtMYB11* (–1220 to –21 bp from the ATG start codon) fused to the β-*glucuronidase* reporter gene (*pAtMYB11::GUS*, Fig. 3). GUS staining was detected from the torpedo (not shown) to the mature embryo stage (Fig. 3A). In 4-d-old seedlings

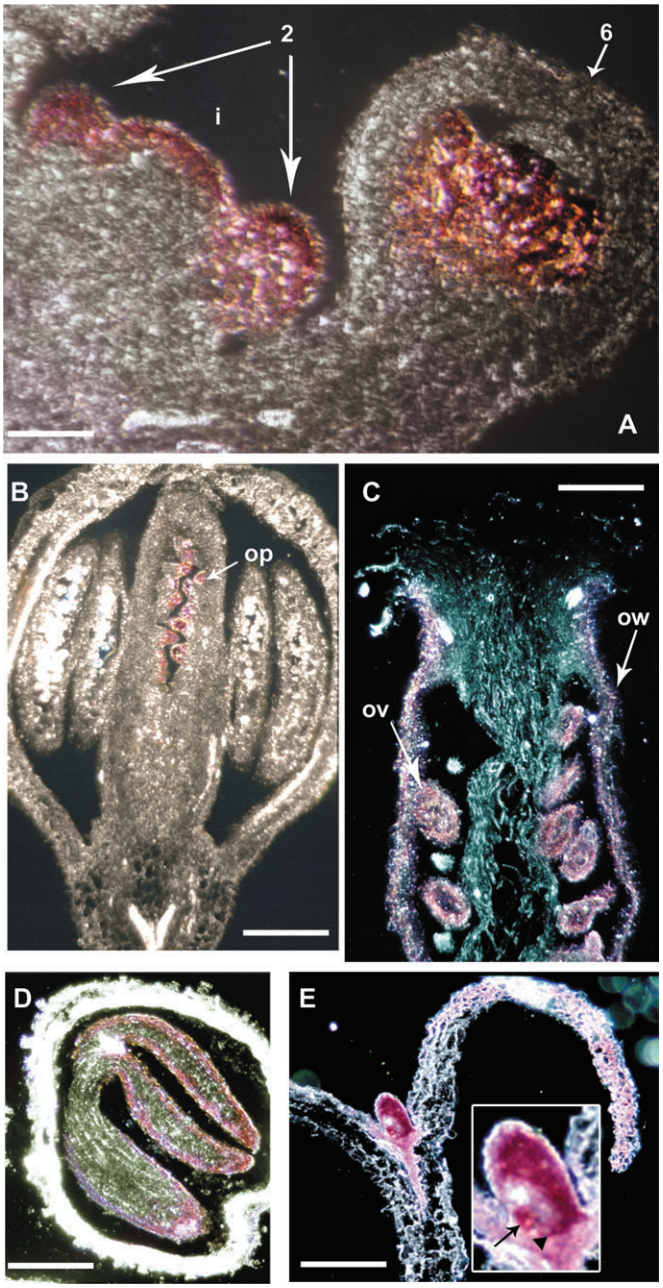

Fig. 2. *In situ* analyses of *AtMYB11* expression. (A) Longitudinal section of inflorescence, showing *AtMYB11* expression in inflorescence meristem (i), floral meristems (2) and in a flower primordium, except sepals (6). Numbers refer to the stage of flower development (Smyth *et al*., 1990). (B) Longitudinal section of flower at stage 10. op, developing ovule primordia. (C) Longitudinal section of the ovary in a flower at stage 13. ov, fertilized ovules developing into seeds; ow, ovary wall developing into silique wall. (D) Mature embryo in seed. (E) Longitudinal section of a 4-d-old seedling, showing *AtMYB11* expression in the shoot apex and cotyledons. Inset, 2.5× magnification of the shoot apex showing *AtMYB11* expression in SAM (arrowhead) and leaf primordium (arrow). For visualizing the red hybridization signal, sections were viewed under dark-field conditions. Bars: (A) 60 μm; (B) 250 μm; (C) 200 μm; (D) 185 μm; (E) 100 μm.

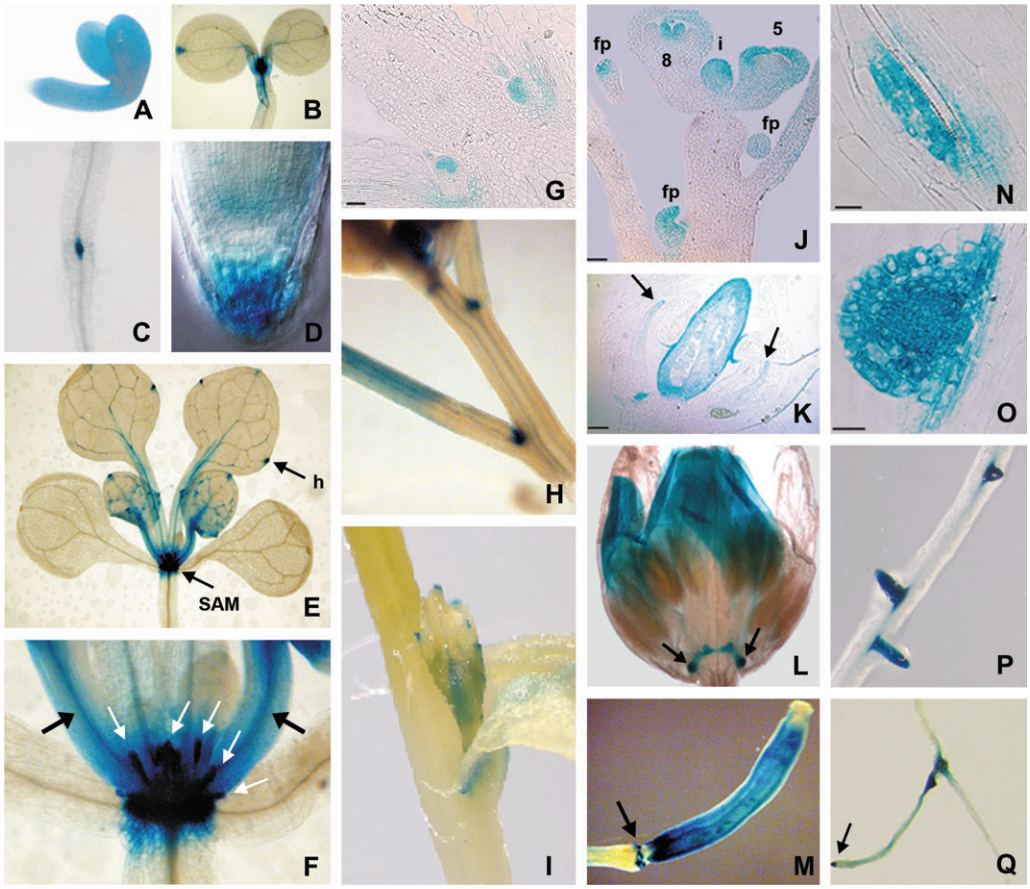

Fig. 3. GUS staining in *pMYB11::GUS* plants. GUS staining in excised mature embryo (A), in the shoot apical meristem (SAM) and cotyledonary tips (B), in an adventitious root meristem (C), in the root apical meristem and columella cells (D, Nomarski image) of a 4-d-old seedling. (E, F) 10-d-old seedling showing expression in shoot apical meristem (SAM) and leaf hydathodes (h) (E), axillary vegetative meristems (white arrows) and procambium of leaf petioles (black arrows) (F). (G–I) GUS activity in axillary meristems at the base of the inflorescence stem (G), in the axil of stem branches (H), and in an axillary inflorescence (I). (J) Longitudinal section of inflorescence showing GUS staining in an inflorescence meristem (i), flower primordia (fp), sepals of flower at stage 5 and in developing gynoecium of flower at stage 8. Numbers refer to the stage of flower development (Smyth *et al*., 1990). (K) Longitudinal section of flower at stage 10, with GUS staining in developing petals (arrows), ovules and in the developing ovary wall. (L) Flower bud showing GUS staining in nectaries (arrows) and petals. (M) Developing silique showing staining in the abscission zone (arrow) and wall. (N–Q) GUS staining in dividing pericycle cells of primary root (N), lateral root dome (O), lateral root primordia after protrusion (P), forking region and root apical meristem (arrow) of a lateral root (Q). Bars: (G, K, N, O) 20 μm; (J) 50 μm.

GUS staining was present in the SAM and at the tip of cotyledons (Fig. 3B). It was also present in the root tip (RAM and columella; Fig. 3D) and in adventitious root meristems (Fig. 3C). In 10-d-old plants, strong GUS staining was present in axillary vegetative meristems (Fig. 3E, F). Leaf primordia were also intensely stained, but as leaf development proceeded, GUS staining declined, becoming progressively confined towards the base until it was visible only in still-developing hydathodes and in the procambium of the petiole (i.e. where meristematic and dividing cells are present) (Fig. 3E, F).

After floral transition, GUS staining was present in the axillary meristems of rosette leaves and stems, and in procambium at their bases (Fig. 3G, H). The pattern of GUS expression in axillary meristems during the development of secondary inflorescences and individual flowers was the same as in the SAM (Fig. 3I).

During flower development, GUS staining was found in all floral organ primordia (sepals, petals, stamens, and carpels) until they showed meristematic features and division activity (Fig. 3J). At stage 10 of flower development, GUS expression was present in developing ovules, ovary walls, and petals (Fig. 3K) and also in developing nectaries at the base of the flower (Fig. 3L). After anthesis, GUS staining was strong in the abscission zone and in the valves of developing siliques (Fig. 3M).

Plants in all developmental stages had GUS staining at the sites of lateral root formation (i.e. in dividing pericycle cells) (Fig. 3N). Strong activity was also present in protruding root domes (Fig. 3O). Root primordia also remained strongly stained after protrusion (Fig. 3P), but later GUS expression became restricted to their procambium, forking region, and root tip (arrow in Fig. 3Q). In all, the GUS expression results corroborate the results

of the *in situ* analyses and show that *AtMYB11* is expressed almost exclusively in meristems and other actively dividing meristematic cells.

The atmyb11-I *mutant grows faster than wild type*

To determine the function of *AtMYB11*, a knock-out mutant, *atmyb11-I*, previously isolated in the *Landsberg erecta* (*Ler*) ecotype was analysed by PCR screening of the Wageningen *En-I* lines, in which the *I* defective transposon is inserted into the R3 repeat of the MYB domain (Meissner *et al*., 1999) (Fig. 1B).

Southern blot analyses revealed the presence of at least four additional *I* insertions in *atmyb11-I* (Fig. 1C). RT-PCR analysis performed on 4-d-old seedlings showed that the *AtMYB11* transcript was not detectable in homozygous *atmyb11-I* individuals (Fig. 1D).

The *atmyb11-I* mutant was morphologically similar to *Ler* plants except that it germinated and grew faster than *Ler* plants. Thus, 2 d after sowing about 50% of *atmyb11-I* seeds had germinated compared to 20% of *Ler* seeds (Fig. 4A). Considering plants germinated at the same time, i.e. on the same day after germination (DAG), a first peak in hypocotyl elongation already occurred at 1.5 d in *atmyb11-I* seedlings and was followed by another one, of similar value, at 2.5 d (Fig. 4B). By contrast, in *Ler* seedlings the first peak occurred at 2 d, and a second similar peak at 3 d and they were both significantly (P <0.01) lower than the two peaks occurring in *atmyb11-I* seedlings (Fig. 4B). The growth of the hypocotyl continued to be significantly (P <0.01) faster in *atmyb11-I* than in *Ler* up to 3.5 d (Fig. 4B). Subsequently, hypocotyl elongation was completed in the *atmyb11-I* mutant, whereas it slowly continued in *Ler* seedlings (Fig. 4B). As a consequence, the final length of the organ was reached in *atmyb11-I* three days earlier than in *Ler* seedlings, and it was not significantly different in the two genotypes (i.e., 2.7±0.02 and 2.2±0.02 mm, respectively).

Also the elongation of the primary root was accelerated in *atmyb11-I* plants (Fig. 5A). In fact, seedlings of both genotypes showed peaks in elongation rate at the same times (i.e. at 1 d and 2.5 d), but those of *atmyb11-I* were significantly (P <0.01) higher (Fig. 5A). Interestingly at 5 d, the root apex (measured including the division zone and excluding the root cap) was significantly longer (P <0.01) in the *atmyb11-I* seedlings than in *Ler* (i.e. 405±10.5 μm and 320.1±10.1 μm, respectively).

Initiation of lateral and adventitious roots was also increased in *atmyb11-I* plants compared to *Ler* (Figs 5C, 6E, F). Two lateral root primordia were formed in 5-d-old *atmyb11-I* seedlings, whereas no root primordia were visible in *Ler* seedlings (Fig. 5C). Seven days after germination *atmyb11-I* plants had more and longer lateral and adventitious roots than in *Ler* plants (Fig. 6E, F). Moreover, the difference in lateral root formation per day

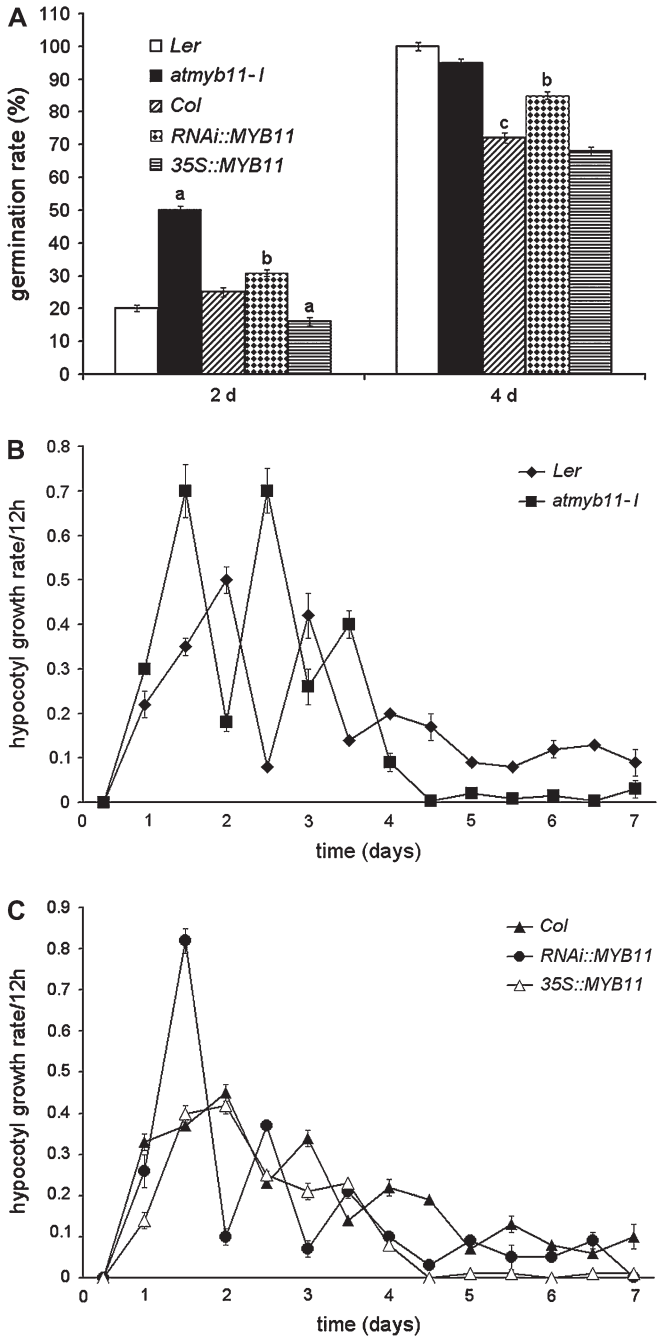

Fig. 4. Analysis of germination and hypocotyl growth rate. (A) Mean percentage of germinated seeds 2 d and 4 d after sowing in *atmyb11-I* mutant, and its wild type *Landsberg erecta* (*Ler*), and in *RNAi::MYB11* and *35S::MYB11* genotypes, and their wild type *Columbia* (*Col*); n=150. (B, C) Hypocotyl growth rate evaluated as mean increases in hypocotyl length at 12 h intervals in seedlings at 0–7 DAG; n=90. In (B) the hypocotyl growth of *atmyb11-I* seedlings in comparison with its wild type *Landsberg erecta* (*Ler*). In (C) hypocotyl growth of *RNAi::MYB11* and *35S::MYB11*seedlings in comparison with their wild type *Columbia* (*Col*). Mean percentages were compared using the Student t test at the same day after germination. a, Significantly different to the corresponding wild-type (*Ler* or *Col*) at P <0.01. b, Significantly different to *Col* and *35S::MYB11* at P <0.01. c, Significantly different to *35S::MYB11* at P <0.05. Bars represent SE, when not shown they are too small to be seen.

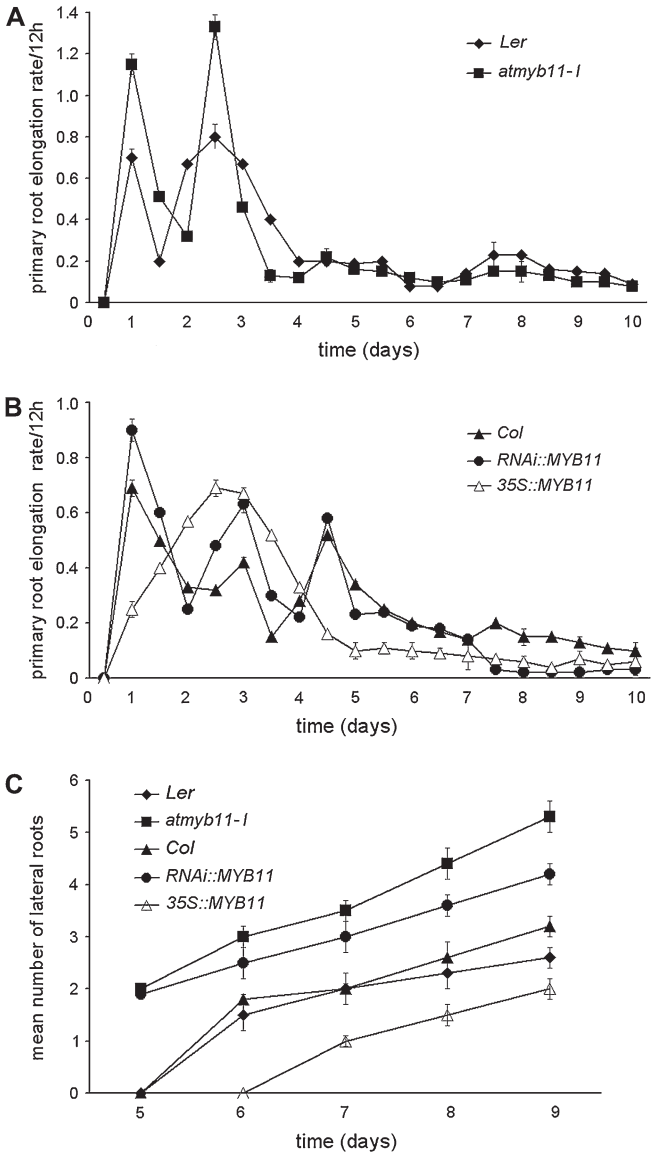

Fig. 5. Primary root elongation rate and lateral root formation. (A, B) Mean increases in primary root length in plants monitored at 12 h intervals from 0–10 DAG; n=90. In (A) root growth of *atmyb11-I* seedlings in comparison with its wild type *Landsberg erecta* (*Ler*). In (B) root growth of *RNAi::MYB11* and *35S::MYB11*seedlings in comparison with their wild type *Columbia* (*Col*). (C) Mean number of lateral roots per day from day 5 to day 9 after germination; n=90. Bars represent SE, when not shown they are too small to be seen.

remained constant up to day 9 (Fig. 5C) and this resulted on day 10, when *atmyb11-I* primary roots were not significantly longer than *Ler* roots (i.e. 16.0±0.1 mm and 14.4±0.5 mm, respectively), into an enhanced number of lateral roots in *atmyb11-I* compared to *Ler* (Table 1), indicating a higher induction of root meristems per root length unit.

Furthermore, after 2 DAG *atmyb11-I* seedlings exhibited two leaf primordia, whereas no primordia were visible in *Ler* seedlings (Fig. 7A). The initiation of leaf primordia was highly accelerated in *atmyb11-I* compared to *Ler* plants up to day 9 (Fig. 7A, P <0.01) and in particular between days 2 and 4 (Figs 7A, 6A, B). There was no significant difference between *atmyb11-I* and *Ler* in terms of number of rosette leaves that developed prior to floral transition (i.e. eight leaves on average were produced by each genotype before floral transition). However, as a consequence of the faster leaf production rate per day, the mutant plants reached the leaf number necessary to floral transition at day 10 (Table 1), i.e. about two days before *Ler*.

In addition, bolting and floral dome production occurred earlier in the mutant compared with *Ler* plants of the same age, as shown by the histological analysis on 12-d-old plants (Fig. 6I, J). On day 17, 11±1.0% of *atmyb11-I* plants showed macroscopic bolting, whereas only 4±0.5% of *Ler* plants had bolted. The difference in the percentage of bolted plants per day remained quite constant up to day 19, but at 21 DAG 74.3±1.6% of *atmyb11-I* plants had bolted inflorescences macroscopically visible compared with 55.6±1.4% of *Ler* plants (Fig. 7B, P <0.05).

At 32 DAG the difference in the percentage of bolted *atmyb11-I* and *Ler* plants was not significant, but *atmyb11-I* stems were longer and had more internodes than *Ler* stems (Table 2) and more *atmyb11-I* plants were fruiting (90.7% versus 63.3%). Siliques were shorter and contained fewer seeds than in *Ler* (Table 3).

AtMYB11 *overexpression reduces growth rate*

To confirm that faster growth was due to inactivation of the *AtMYB11* gene, two independent transgenic lines (*RNAi::MYB11*), showing a complete absence of the *AtMYB11* transcript and two lines (*35S::MYB11*) showing elevated expression levels of the *AtMYB11* gene under the control of the *CaMV35S* promoter were selected (data not shown). Both types of transgenics were similar in appearance to *Columbia* (*Col*) wild-type plants, but the constructs had opposing effects on germination and growth rate.

As was the case with the *atmyb11-I* mutant in comparison with *Ler*, significantly more *RNAi::MYB11* seeds than *Col* seeds had germinated 2 d and 4 d after sowing (Fig. 4A). Shoot and root development in *RNAi::MYB11* was faster than in *Col*. In fact, a main peak in hypocotyl elongation of *RNAi::MYB11* seedlings has already been observed at 1.5 d, followed by a second lower peak at 2.5 d, whereas the two peaks occurred later in *Col* (i.e. at 2 d and 3 d) and were both significantly (P <0.01) lower than the first one of *RNAi::MYB11* seedlings (Fig. 4C). However, the final length of the organ was not significantly different (i.e. 2.3±0.5 mm and 2.0±0.5 mm, respectively). Primary root elongation showed three peaks of growth in *RNAi::MYB11* seedlings which were contemporary to those in *Col*, but the first and the third were significantly (P <0.01) higher (Fig. 5B).

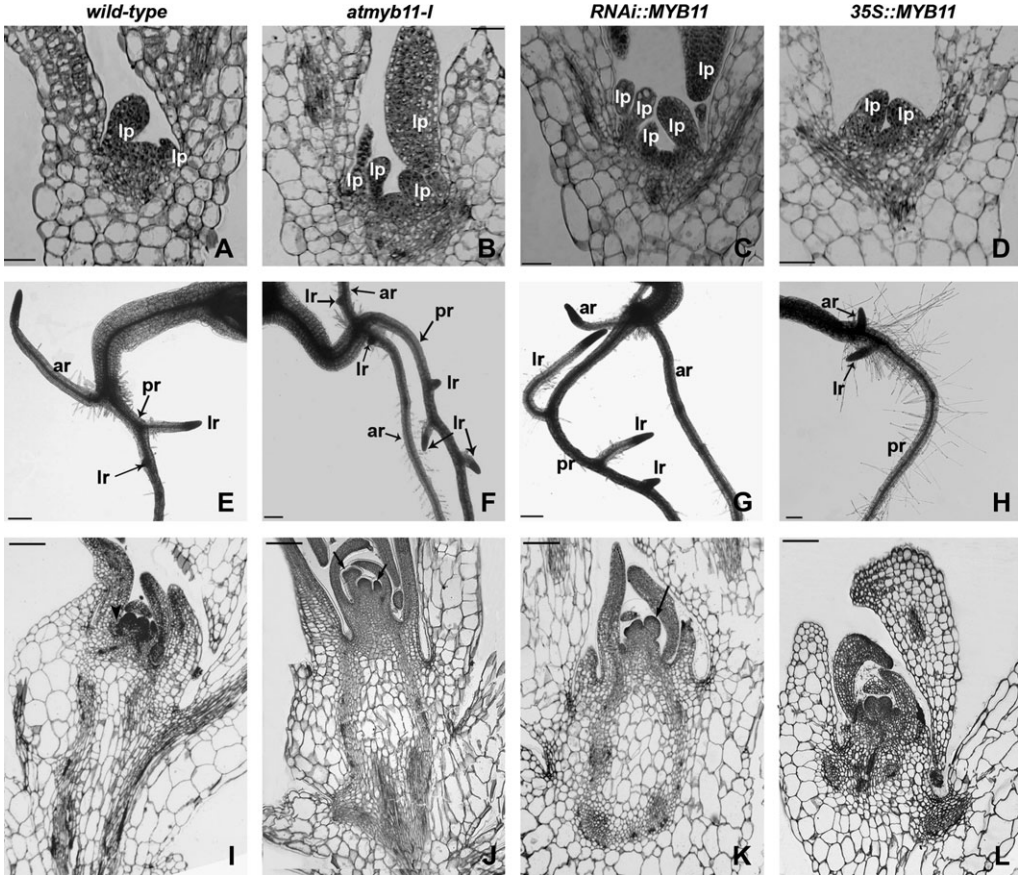

Fig. 6. Shoot, root, and inflorescence apex development. (A–D) Longitudinal sections of SAM in 4-d-old seedlings. Bars, 50 μm. (E–H) Root systems of 7-d-old seedlings. Bars, 200 μm. (I–L) Longitudinal sections of the inflorescence apex in 12-d-old seedlings. Bars, 100 μm. (A, E, I) *Landsberg erecta* ecotype; (B, F, J) *atmyb11-I*; (C, G, K) *RNAi::MYB11*; (D, H, L) *35S::MYB11*. ar, adventitious root; lp, leaf primordium; lr, lateral root; pr, primary root. Arrowheads indicate emerging floral meristems; arrows indicate floral domes.

Similarly to *atmyb11-I* seedlings, the root apex in 5-d-old *RNAi::MYB11* seedlings was significantly longer (P <0.01) than in *Col* (i.e. 421.4±13.7 μm and 295.1±9.6 μm, respectively). Initiation of lateral and adventitious roots in *RNAi::MYB11* was also accelerated as in *atmyb11-I* plants (Figs 5C, 6F, G). Considering that the length of *RNAi::MYB11* primary roots at day 10 was the same as in *Col* plants (i.e. 10.1±0.2 mm and 10.8±0.3 mm, respectively), lateral root formation was also significantly enhanced in *RNAi::MYB11* with respect to *Col* (Table 1).

The initiation of rosette leaves per day was accelerated as in *atmyb11-I* mutant (Fig. 6B, C), i.e. at day 4, there were 3-fold more leaf primordia in *RNAi::MYB11* seedlings than in *Col* (Fig. 7A).

By contrast, *35S::MYB11* seeds germinated more slowly than *Col* (Fig. 4A) and seedlings had significantly (P <0.01) shorter hypocotyls (1.4±0.2 mm), roots (4.9±0.4 mm), and root apex (i.e. 190.5±17.7 μm at day 5) compared to *Col*. Furthermore, the hypocotyl and primary root elongation rates showed only one peak of growth (i.e. at 2 d and 2.5 d, respectively), and a reduced growth period, i.e. about four days (Figs 4C, 5B).

Table 1. *Number of rosette leaves and of lateral and adventitious roots*

The number of rosette leaves and of lateral and adventitious roots per primary root was determined in 10-d-old seedlings of *atmyb11-I*, *RNAi::MYB11*, and *35S::MYB11* plants compared to wild type (*Ler* for *atmyb11-I*; *Col* for *RNAi::MYB11* and *35S::MYB11*) and expressed as mean values ±SE. At day 10, *atmyb11-I* and *RNAi::MYB11* plants were at floral transition, whereas *35S::MYB11*, *Ler* and *Col* were still vegetative. Means were compared using Student *t* test.

Genotypes	Rosette leaves	Lateral roots	Adventitious roots
Ler	6.5±0.3	3.0±0.3	1.3±0.2
atmyb11-I	7.9±0.2[a]	6.2±0.3[a]	2.0±0.1[a]
Col	6.6±0.1	3.9±0.1	1.1±0.1
RNAi::MYB11	7.5±0.4[b]	4.9±0.2[b]	1.8±0.2[b]
35S::MYB11	6.0±0.2[c]	2.6±0.6[c]	1.0±0.2

[a] Significantly different to *Ler* at $P < 0.01$.
[b] Significantly different to *Col* and *35S::MYB11* at P <0.01.
[c] Significantly different to *Col* at P <0.05; (n=30).

Four days after germination the number of leaf primordia of *35S::MYB11* (i.e. 2±1.0; Fig. 6D) was the same as in *Col* (Figs 6D, 7A), but at later times there were

fewer rosette leaves and fewer lateral roots in the *35S::MYB11* plants (Fig. 6H; Table 1).

At 12 DAG, the inflorescence apex of *RNAi::MYB11* plants showed histologically the onset of bolting and the production of floral domes, showing an acceleration in development similar to *atmyb11-I* plants (Fig. 6K, J). By contrast, *35S::MYB11* (Fig. 6L) and *Col*, similarly to *Ler* plants (Fig. 6I), exhibited only the inception of floral meristems.

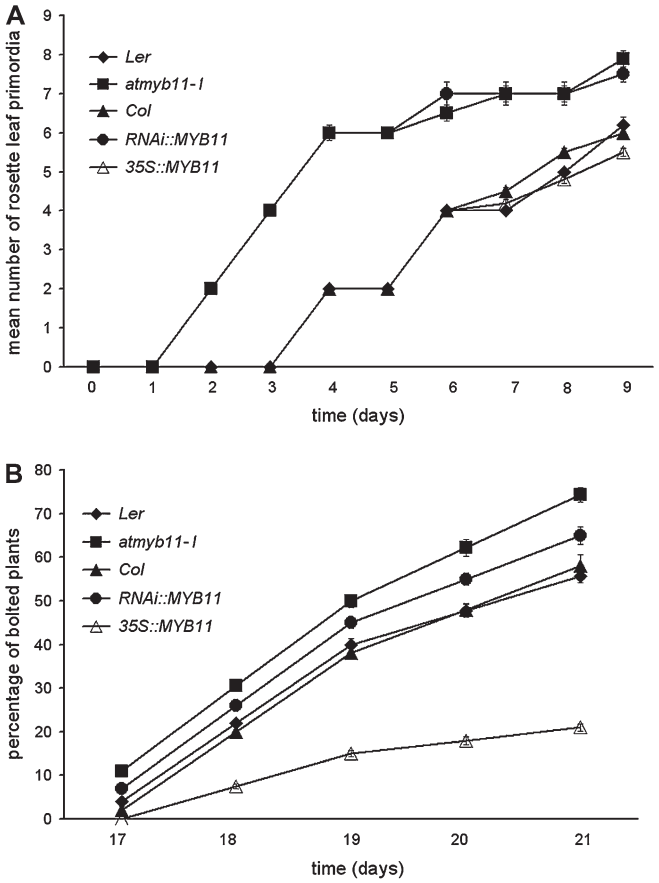

Fig. 7. Analysis of the formation of rosette leaves, and floral bolting in *atmyb11-I* mutant, and its wild type *Landsberg erecta* (*Ler*), and in *RNAi::MYB11* and *35S::MYB11* genotypes, and their wild type *Columbia* (*Col*). (A) Mean number of rosette leaf primordia at 0–9 DAG; n=90. (B) Mean percentage of plants showing macroscopic bolting after floral transition evaluated daily from 17 DAG to 21 DAG; n=90. Bars represent SE.

As for *atmyb11-I* plants, macroscopic bolting initiated at day 17 in *RNAi::MYB11* plants, whereas it was occasional in *Col* (Fig. 7B). Again as for *atmyb11-I* plants, the difference in the percentage of *RNAi::MYB11* and *Col* bolted plants was constant up to day 21, when 65±2% of *RNAi::MYB11* plants had bolted inflorescences macroscopically visible compared to 58±2.6% of *Col* plants (Fig. 7B; P <0.05). At day 32, the percentage of *RNAi::MYB11* bolted plants was not significantly different than in *Col*, similarly to *atmyb11-I* and *Ler* plants (Table 2). Bolting in *35S::MYB11* plants was rather scarce (Fig. 7B), resulting at day 32 in 30±1.2% of *35S::MYB11* bolted plants, i.e. less than half compared to *Col* and *RNAi::MYB11* (Table 2). In addition, *35S::MYB11*plants exhibited significantly shorter stems, and fewer internodes and flowers than *Col* and *RNAi::MYB11* plants (Table 2). The number of siliques was reduced in *35S::MYB11* and enhanced in *RNAi::MYB11* plants compared to *Col* (Table 2). However, siliques of both genotypes were similarly shorter and contained fewer seeds than *Col*, but the number of seeds was much more reduced in *35S::MYB11* than in *RNAi::MYB11* (Table 3).

Root formation in vitro *is enhanced in atmyb11-I* and reduced in *35S::MYB11*

To evaluate the effects of *AtMYB11* on the morphogenic potential of tissues, thin cell layer (TCL) explants were obtained from stems of *atmyb11-I*, *Ler*, *35S::MYB11*, and *Col* plants and cultured on a root-inducing medium.

The formation of adventitious roots occurred in thin cell layers (TCLs) of 35-d-old plants of all genotypes. However, *Col* and *Ler* explants showed a similar rooting response, as shown in Fig. 8A for *Ler*, whereas differences

Table 2. *Inflorescence height and number of internodes, flowers, and siliques*

Mean percentage of bolted plants and mean inflorescence height, number of internodes, flowers, and siliques (±SE) were determined at 32 DAG. Inflorescence height was evaluated as length of primary stem. Measurements were done on *atmyb11-I*, *RNAi::MYB11*, and *35S::MYB11* plants compared to wild type (*Ler* for *atmyb11-I*; *Col* for *RNAi::MYB11* and *35S::MYB11*). Means were compared using Student t test. n=60.

	Ler	*atmyb11-I*	*Col*	*RNAi::MYB11*	*35S::MYB11*
Bolted plants (%)	83.3±2.8	93.3±2.9	70.0±1.9	80.0±2.0	30.0±1.2[a]
Inflorescence height (cm)	7.4±0.4	9.7±0.3[b]	15.5±0.5	16.7±0.5	10.0±0.4[a]
No. of internodes	3.2±0.2	3.9±0.1[b]	8.0±0.2	8.7±0.2	3.4±0.5[a]
No. of flowers	nd[e]	nd[e]	3.0±0.2	3.0±0.2	2.0±0.3[c]
No. of siliques	nd[e]	nd[e]	6.1±0.4	8.2±0.5[d]	3.3±0.6[a]

[a] Significantly different to *Col* and *RNAi::MYB11* at P <0.01.
[b] Significantly different to *Ler* at P <0.01.
[c] Significantly different to *Col* and *RNAi::MYB11* at P <0.05.
[d] Significantly different to *Col* at P <0.05.
[e] nd, Not determined.

in the response of *atmyb11-I* (Fig. 8C) and *35S::MYB11* (Fig. 8E) TCLs were observed compared to the corresponding wild type (Fig. 8A). In fact, the mean percentage of root-forming TCLs of *atmyb11-I* plants was significantly (P <0.01) higher than that of *Ler* (i.e. 90.6±3.5 and 62.9±4.8, respectively), whereas that of *35S::MYB11* TCLs was significantly (P <0.01) lower than that of *Col* (i.e. 50.6±2.8 and 74.5±3.8, respectively). Furthermore, *atmyb11-I* TCLs were the only explants that appeared totally covered by roots at the end of culture (compare Fig. 8C with Fig. 8A and E). Furthermore, the histological analysis showed that *atmyb11-I* TCLs exhibited less callus and a higher density of root meristemoids and primordia compared to wild-type TCLs (Fig. 8D, B), whereas *35S::MYB11* TCLs showed a very low formation of root meristemoids and primordia (Fig. 8F), thus indicating that the silencing of the *AtMYB11* gene increases *de novo* formation of meristemoids in the explants, whereas the overexpression of *AtMYB11* has an opposite effect.

Discussion

It has been shown that the *AtMYB11* gene is expressed at all developmental stages and in all organs of *Arabidopsis*, and that it is confined to actively dividing meristematic cells. Specifically, the *AtMYB11* gene was expressed during embryogenesis, in primary, lateral, and adventitious meristems, and in the still meristematic leaf, root, and floral organ primordia. Interestingly, in young leaf primordia, the expression pattern of *AtMYB11* showed a basipetal gradient similar to that of cell division activity. In fact, the outgrowth of leaf primordia and formation of the leaf blade are driven by cell proliferation until the size of a primordium of a few millimetres is reached, after which a progressive cessation of cell division proceeds from the distal tip towards the base (Donnelly *et al*., 1999; Fleming, 2002). Later on in mature organs, the *AtMYB11* transcript was abundant in the cells which had reprogrammed to generate meristemoids giving rise to hydathodes and nectaries.

Table 3. *Size of siliques and number of seeds per silique*

Size of mature siliques and number of seeds were determined at 40 DAG from *atmyb11-I*, *RNAi::MYB11*, and *35S::MYB11* plants compared to wild type (*Ler* for *atmyb11-I*; *Col* for *RNAi::MYB11* and *35S::MYB11*), expressed as mean values (±SE) and compared using Student *t* test. n=30.

	Ler	*atmyb11-I*	*Col*	*RNAi::MYB11*	*35S::MYB11*
Length (μm)	8.3±0.4	6.6±0.2[a]	12.3±0.4	10±0.4[c]	10.5±0.3[c]
Width (μm)	0.97±0.12	0.95±0.11	0.97±0.2	0.97±0.3	0.95±0.3
No. of seeds	27.4±1.5	23.2±1.3[b]	30±0.3	25±0.4[d]	19.6±0.3[c]

[a] Significantly different to *Ler* at P <0.01.
[b] Significantly different to *Ler* at P <0.05.
[c] Significantly different to *Col* at P <0.01.
[d] Significantly different to *Col* and *35S::MYB11* at P <0.01.

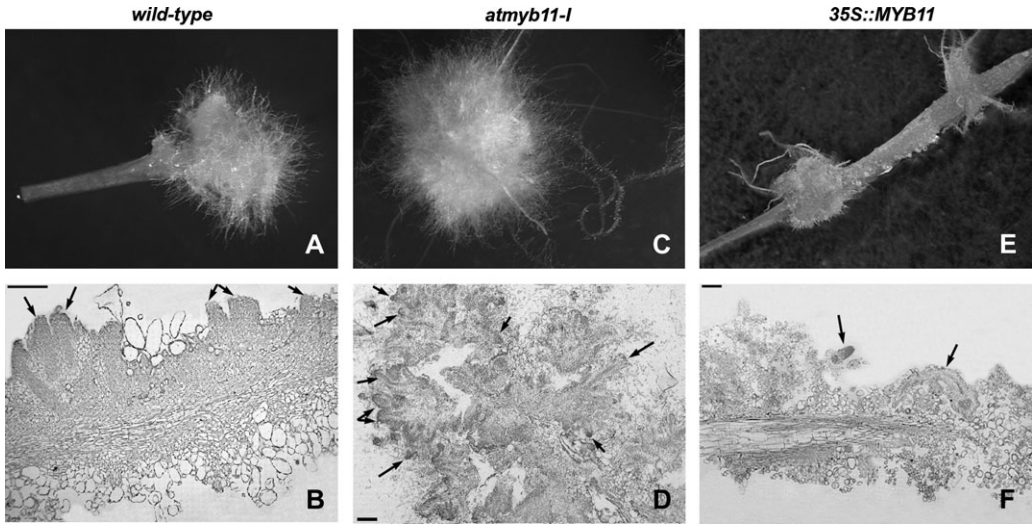

Fig. 8. Adventitious root formation from TCLs excised from the inflorescence stem of 35-d-old *Ler* (A, B), *atmyb11-I* (C, D), and *35S::MYB11* (E, F) plants and cultured for 30 d on a rooting medium in darkness. (A, C, E) macroscopic response, (B, D, F) histological longitudinal sections (bars=100 μm). Arrows indicate root primordia.

Mutated plants (*atmyb11-I* and *RNAi::MYB11*) not expressing the *AtMYB11* gene were characterized by faster germination and faster vegetative growth. This acceleration of growth continued after floral transition, resulting in plants with taller stems, and more internodes and siliques. The opposite phenotype was displayed by *35S::AtMYB11* plants that overexpress *AtMYB11*. Plant development is generally due to a balance between cell division in meristematic tissues to produce tissues/organs and cell growth and differentiation to allow organ development and maturation. Since initiation and early growth of leaf primordia involves both cell proliferation within the primordium and recruitment of cells from the meristem, a faster initiation of leaf primordia would result in a shoot meristem depleted of stem cells, if its cells were not replenished at the same rate of leaf initiation. As a consequence, a reduction in leaf number may also be observed. Since the number of rosette leaves produced prior to bolting remained unaltered, the faster initiation of leaf primordia observed in *atmyb11-I* and *RNAi::MYB11* plants suggests that the inactivation of *AtMYB11* may cause an accelerated cell production rate in the SAM and in the early primordium. Similar conclusions can be drawn for the root, where the accelerated cell production rate in RAM had already resulted into a more extended root apex in *atmyb11-I* and *RNAi::MYB11* primary roots at day 5. In addition, a faster initiation rate of lateral and adventitious roots, but no alterations in overall root morphology and length, or in the pattern of initiation was observed. These findings suggest that *AtMYB11* may control growth along the longitudinal axis of the plant possibly by reducing the cell production rate in SAM, RAM, and axillary lateral and adventitious meristems, without discriminating between initial and derivative cells and being active in lateral/adventitious organ primordia until proliferation activity is present.

In *Arabidopsis*, floral transition in the SAM is followed by bolting of the stem and the phenotype of the early flowering mutants is characterized by a reduction in rosette leaf number in comparison with the wild type. It is shown that the lines with inactivated *AtMYB11* reached the bolting stage faster than both wild type and *AtMYB11* overexpressing lines, but this was a consequence of an overall faster growth and not of an earlier floral transition, since no difference in the number of rosette leaves was found. Furthermore, the differences in flower and silique number after 32 d of growth between *RNAi::MYB11* and *35S::AtMYB11* lines compared to wild type may also be due to a different rate of cell division in the inflorescence and floral meristems. It is not clear how both loss of *AtMYB11* expression and its overexpression may lead to shorter siliques with less seeds than wild-type, since many factors affect reproduction and fertility. However, some examples of mutants are known in which a delayed growth is associated to reduced silique size and seed set, as observed for *35S::MYB11* (Huang *et al*., 2001; Himanen *et al*., 2003; Yang *et al*., 2007). On the other hand, in mutated plants (*atmyb11-I* and *RNAi::MYB11*) an energy imbalance might cause a reduced silique size and seed production, since the additional lateral outgrowths (flowers/fruits) are additional sinks for nutrients.

The role of *AtMYB11* in reducing the production rate of meristematic cells is further sustained by the results of TCL experiments. The cells of the TCLs are excised from the epidermal and cortical layers of an adult organ, i.e. stem, and are totally reprogrammed by the hormones added to the culture medium for proliferating into a callus and producing the root meristems *de novo* (Falasca *et al*., 2004). The enhancement of root meristemoid formation observed in the knock-out *atmyb11-I* explants (not associated with an enhanced callus proliferation) and the reduced number of neoformed meristemoids observed in the explants from *35S::MYB11* plants compared to wild type demonstrate that *AtMYB11* plays a meristem-inhibiting action in TCL explants. Since it has been demonstrated that the development of neoformed meristemoids and organs on TCLs is comparable with that observed *in planta* (Altamura *et al*., 1991; Falasca and Altamura, 2003; Falasca *et al*., 2004), these results probably reflect the role played by *AtMYB11 in planta*.

Accelerated growth is typically associated with alterations in cell cycle genes in meristems. Indeed, preliminary results suggest that the silencing of *AtMYB11* determines a change in the timing of expression of cell cycle genes, for example, *AtCYCD2;1*, *AtCYCB1;1*, and *AtCDKA;1* (Doerner *et al*., 1996; Cockcroft *et al*., 2000; Beemster *et al*., 2002). However, an in-depth analysis of germinating seedlings and developing plants is necessary to unravel how the expression of these and other cell cycle genes is locally affected in different meristems and primordia, when the *AtMYB11* expression is altered.

Recently, the analysis of the closely related *MYB* genes, *AtMYB11*, *AtMYB12*, and *AtMYB111*, has been reported showing that, in developing seedlings *AtMYB12* and *AtMYB111* are mainly responsible for the control of flavonol biosynthesis in roots and cotyledons, respectively, but no significant differences in flavonol accumulation were detected in their *atmyb11* mutant compared with wild type (Stracke *et al*., 2007). Based on the results here presented, we propose that *AtMYB11* controls the rate of germination and modulates growth in *Arabidopsis* by reducing proliferation activity in the meristematic cells. Further studies are required to identify the direct targets of *AtMYB11* and to determine how the timing and extent of expression of these targets are controlled during germination and throughout plant development.

Acknowledgements

The authors thank Martin Kater for helpful discussions, and Don Ward and Ann Elizabeth Errico for English revision. This work was

supported by the Italian Ministry of Universities and Research (FIRB), European Union grant QLRT-1999-876 to CT, and by Progetti Ateneo of the Università La Sapienza to MMA.

References

Aarts MG, Corzaan P, Stiekema WJ, Pereira A. 1995. A two-element *Enhancer-Inhibitor* transposon system in *Arabidopsis thaliana*. *Molecular and General Genetics* **247,** 555–564.

Altamura MM, Capitani F, Serafini-Fracassini D, Torrigiani P, Falasca G. 1991. Root histogenesis from tobacco thin cell layers. *Protoplasma* **161,** 31–42.

Becker D, Kemper E, Schell J, Masterson R. 1992. New plant binary vectors with selectable markers located proximal to the left T-DNA border. *Plant Molecular Biology* **20,** 1195–1197.

Beemster GT, De Vusser K, De Tavernier E, De Bock K, Inzé D. 2002. Variation in growth rate between Arabidopsis ecotypes is correlated with cell division and A-type cyclin-dependent kinase activity. *Plant Physiology* **129,** 854–864.

Berlyn MB, Last RL, Fink GR. 1989. A gene encoding the tryptophan synthase beta subunit of *Arabidopsis thaliana*. *Proceedings of the National Academy of Sciences, USA* **86,** 4604–4608.

Byrne ME, Barley R, Curtis M, Arroyo JM, Dunham M, Hudson A, Martienssen RA. 2000. *Asymmetric leaves1* mediates leaf patterning and stem cell function in Arabidopsis. *Nature* **408,** 967–971.

Clough SJ, Bent AF. 1988. Floral dip: a simplified method for *Agrobacterium*-mediated transformation of *Arabidopsis thaliana*. *The Plant Journal* **16,** 735–743.

Cockcroft CE, den Boer BG, Healy JM, Murray JA. 2000. Cyclin D control of growth rate in plants. *Nature* **405,** 575–579.

Coen ES, Romero JM, Doyle S, Elliott R, Murphy G, Carpenter R. 1990. *floricaula*: a homeotic gene required for flower development in *Antirrhinum majus*. *Cell* **63,** 1311–1322.

Cominelli E, Galbiati M, Vavasseur A, Conti L, Sala T, Vuylsteke M, Leonhardt N, Dellaporta SL, Tonelli C. 2005. A guard-cell-specific MYB transcription factor regulates stomatal movements and plant drought tolerance. *Current Biology* **15,** 1196–1200.

Dellaporta S, Moreno M. 1994. Southern blot hybridization. In: Freeling M, Walbot V, eds. *The maize handbook*. New York, Berlin, Heidelberg: Springer, 569–572.

Doerner P, Jorgensen JE, You R, Steppuhn J, Lamb C. 1996. Control of root growth and development by cyclin expression. *Nature* **380,** 520–523.

Donnelly PM, Bonetta D, Tsukaya H, Dengler RE, Dengler NG. 1999. Cell cycling and cell enlargement in developing leaves of Arabidopsis. *Developmental Biology* **215,** 407–419.

Falasca G, Altamura MM. 2003. Histological analysis of adventitious rooting in *Arabidopsis thaliana* (L.) Heynh seedlings. *Plant Biosystems* **137,** 265–274.

Falasca G, Zaghi D, Possenti M, Altamura MM. 2004. Adventitious root formation in *Arabidopsis thaliana* thin cell layers. *Plant Cell Reports* **23,** 17–25.

Fleming AJ. 2002. The mechanism of leaf morphogenesis. *Planta* **216,** 17–22.

Galbiati M, Moreno MA, Nadzan G, Zourelidou M, Dellaporta SL. 2000. Large-scale T-DNA mutagenesis in Arabidopsis for functional genomic analysis. *Functional and Integrative Genomics* **1,** 25–34.

Gusmaroli G, Tonelli C, Mantovani R. 2001. Regulation of the CCAAT-binding NF-Y subunits in *Arabidopsis thaliana*. *Gene* **264,** 173–185.

Himanen K, Reuzeau C, Beeckman T, Melzer S, Grandjean O, Corben L, Inzé D. 2003. The Arabidopsis locus *RCB* mediates upstream regulation of mitotic gene expression. *Plant Physiology* **133,** 1862–1872.

Hirayama T, Shinozaki K. 1996. A *cdc5+* homolog of a higher plant, *Arabidopsis thaliana*. *Proceedings of the National Academy of Sciences, USA* **93,** 13371–13376.

Huang S, Cerny RE, Bhat DS, Brown SM. 2001. Cloning of an Arabidopsis patatin-like gene, STURDY, by activation T-DNA tagging. *Plant Physiology* **125,** 573–584.

Ito M, Araki S, Matsunaga S, Itoh T, Nishihama R, Machida Y, Doonan JH, Watanabe A. 2001. G_2/M-phase-specific transcription during the plant cell cycle is mediated by c-Myb-like transcription factors. *The Plant Cell* **13,** 1891–1905.

Keller T, Abbott J, Moritz T, Doerner P. 2006. Arabidopsis *REGULATOR OF AXILLARY MERISTEMS1* controls a leaf axil stem cell niche and modulates vegetative development. *The Plant Cell* **18,** 598–611.

Labereke NV, Engler G, Holster J, Elsacker SV, Zaenen J, Schilperoort RA, Schell J. 1974. Large plasmid in *Agrobacterium tumefaciens* essential for crown gall-inducing ability. *Nature* **252,** 169–170.

Malamy JE, Benfey PN. 1997. Organization and cell differentiation in lateral roots of *Arabidopsis thaliana*. *Development* **124,** 33–44.

Meissner RC, Jin H, Cominelli E, Denekamp M, *et al*. 1999. Function search in a large transcription factor gene family in Arabidopsis: assessing the potential of reverse genetics to identify insertional mutations in *R2R3 MYB* genes. *The Plant Cell* **11,** 1827–1840.

Muller D, Schmitz G, Theres K. 2006. *Blind* homologous *R2R3 Myb* genes control the pattern of lateral meristem initiation in Arabidopsis. *The Plant Cell* **18,** 586–597.

Murashige T, Skoog F. 1962. A revised medium for rapid growth and bioassays with tobacco tissue cultures. *Physiologia Plantarum* **15,** 473–497.

Petroni K, Tonelli C, Paz-Ares J. 2002. The MYB transcription factor family: from maize to Arabidopsis. *Maydica* **47,** 213–232.

Planchais S, Perennes C, Glab N, Mironov V, Inzé D, Bergounioux C. 2002. Characterization of *cis*-acting element involved in cell cycle phase-independent activation of *Arath; CycB1;1* transcription and identification of putative regulatory proteins. *Plant Molecular Biology* **50,** 111–127.

Procissi A, Dolfini S, Ronchi A, Tonelli C. 1997. Light-dependent spatial and temporal expression of pigment regulatory genes in developing maize seeds. *The Plant Cell* **9,** 1547–1557.

Schmitz G, Tillmann E, Carriero F, Fiore C, Cellini F, Theres K. 2002. The tomato *Blind* gene encodes a MYB transcription factor that controls the formation of lateral meristems. *Proceedings of the National Academy of Sciences, USA* **99,** 1064–1069.

Smyth DR, Bowman JL, Meyerowitz EM. 1990. Early flower development in Arabidopsis. *The Plant Cell* **2,** 755–767.

Speulman E, Metz PL, van Arkel G, te Lintel Hekkert B, Stiekema WJ, Pereira A. 1999. A two-component enhancer-inhibitor transposon mutagenesis system for functional analysis of the Arabidopsis genome. *The Plant Cell* **11,** 1853–1866.

Stracke R, Ishihara H, Huep G, Barsch A, Mehrtens F, Niehaus K, Weisshaar B. 2007. Differential regulation of closely related R2R3-MYB transcription factors controls flavonol accumulation in different parts of the *Arabidopsis thaliana* seedling. *The Plant Journal* **50,** 660–677.

Stracke R, Werber M, Weisshaar B. 2001. The *R2R3-MYB* gene family in *Arabidopsis thaliana*. *Current Opinion in Plant Biology* **4,** 447–456.

Timmermans MC, Hudson A, Becraft PW, Nelson T. 1999. ROUGH SHEATH2: a Myb protein that represses knox homeobox genes in maize lateral organ primordia. *Science* **284,** 151–153.

Towers MI, Ito M, Roberts G, Doonan JH. 2003. Developmental control of the cell cycle. *Cell Biology International* **27,** 283–285.

Uberlacker B, Werr W. 1996. Vectors with rare-cutter reastriction enzyme sites for expression of open reading frames in transgenic plants. *Molecular Breeding* **2,** 293–295.

van Tunen AJ, Koes RE, Spelt CE, van der Krol AR, Stuitje AR, Mol JN. 1988. Cloning of the two chalcone flavanone isomerase genes from *Petunia hybrida*: coordinate, light-regulated and differential expression of flavonoid genes. *EMBO Journal* **7,** 1257–1263.

Waites R, Selvadurai HR, Oliver IR, Hudson A. 1998. The *PHANTASTICA* gene encodes a MYB transcription factor involved in growth and dorsoventrality of lateral organs in Antirrhinum. *Cell* **93,** 779–789.

Weston K. 1998. Myb proteins in life, death and differentiation. *Current Opinion in Genetics and Development* **8,** 76–81.

Yang J, Sardar HS, McGovern KR, Zhang Y, Showalter AM. 2007. A lysine-rich arabinogalactan protein in Arabidopsis is essential for plant growth and development, including cell division and expansion. *The Plant Journal* **49,** 629–640.

Yanhui C, Xiaoyuan Y, Kun H, *et al.* 2006. The MYB transcription factor superfamily of Arabidopsis: expression analysis and phylogenetic comparison with the rice MYB family. *Plant Molecular Biology* **60,** 107–124.